Adaptive Predictor-Based Sliding PID Uncalibrated Visual Servoing with Uncertain Jacobian for Dynamic Tracking of Robots

§J. D. Fierro-Rojas, †E.C. Dean-León, ¶V. Parra-Vega, and ‡A.Espinosa-Romero
§Industrial Mechatronics Engg. Dept. Ecatepec Institute Technology of Superior Studies – Mexico
†Mechatronics Division - CINVESTAV, México.
¶Center for Advanced Technology - CIATEQ, Retablo 150, Fovissste, Querétaro, 76150 México
‡Institute for Applied Mathematics and Systems - UNAM, México.
Email addresses: {jfierro,edean,vparra}@mail.cinvestav.mx, arturoe@leibniz.iimas.unam.mx.

Abstract—Image acquisition and processing for closed-loop control purposes is known as visual servoing. There are fundamental scientific problems here, the most important perhaps is conceptual, since the image is a static variable in the formulation of the problem. The technological challenges is the time delay induced by the CCD camera itself. In this paper, the experimental validation of a decentralized non-linear PID-like structure of a visual feedback controller under an uncalibrated fixed-camera configuration [7] is addressed in this paper. By using the projection algorithm as an adaptive prediction technique, our scheme evades the time delay problem associated CCD cameras. Additionally, finite-time tracking is ensured provided that a time-base generator models a time-varying feedback gain. Since no regressor is computed and robot dynamics is only considered in the stability analysis, the system is very inexpensive in comparison to the few dynamic visual servoing controllers available in the literature. The high performance of the proposed controller has been tested successfully in real time on a direct drive robot that tracks a desired image-based trajectories, using a IEEE1394 standard camera.

I. INTRODUCTION

To improve the visual servoing performance a compensation of robot dynamics has been considered in the control design. Furthermore, the most significant issues in visual tracking is due to the innate characteristics of the vision sensor which include relatively low refreshing rate, thus provoking latency. The control performance also depends on the quality of the camera calibration [9], which is usually a difficult process prone to error. Thus, these problems have been studied with an uncalibrated camera with unknown robot parameters [2], [3], [4], [8], though, these schemes require knowledge of the manipulator dynamics. On the other hand, adaptive control techniques guarantee asymptotic stability with a considerable on-line computational load of regressor and adaptive parameters. In contrast, [7] presents a regressor free controller which guarantees exponential tracking in image space with fixed camera configuration for 2D image-based tracking.

A. Contribution

The real time performance of the novel dynamical visual servoing scheme [7] is presented and discussed. The salient feature is the simplicity of the decentralized controller, which exhibits a PID-like structure based on image tracking errors. To deal with the latency of the CCD camera, we use a projection algorithm as an adaptive predictor which evades problems of time delay associated to image acquisition and processing. Furthermore, the controller guaranties a finite-time convergence by selecting an explicit time-varying feedback gain, this regime is faster than exponential regime. A rough estimation of the robot Jacobian matrix and camera parameters is required instead of accurate one. Experiments show that even under 99% of uncertainty of these parameters, exponential tracking is obtained.

II. ROBOT MODEL

The dynamics of a serial $n-$link rigid, non-redundant, fully actuated robot manipulator can be written as follows

$$H(q)\ddot{q} + C(q,\dot{q})\dot{q} + g(q) = \tau \qquad (1)$$

where $q \in R^n$ is the vector of generalized joint displacements, with $\dot{q} \in R^n$ its velocity, $\tau \in R^{n \times 1}$ stands for the vector applied joint torques, $H(q) \in$

$R^{n \times n}$ is the symmetric positive definite manipulator inertia matrix, $C(q,\dot{q})\dot{q} \in R^n$ stands for the vector of centripetal and Coriolis torques, and finally $G(q) \in R^n$ is the vector of gravitational torques.

III. CAMERA MODEL

For planar robots, and using thin lens without aberration, [6] presented the widely accepted fixed (static) camera configuration, whose basic mathematical description of this system consists of a composition of four transformations defined as follows

- Joint to Cartesian transformation
- Cartesian to Camera transformation
- Camera to CCD transformation
- CCD to Image transformation

Then the following inverse differential kinematics that relates generalized joint velocities $\dot{q}$ and image velocities $\dot{x}$ appears

$$\dot{q} = J^{-1}R^{-1}\alpha^{-1}\dot{x} \equiv J^{-1}R_\alpha^{-1}\dot{x} \qquad (2)$$

where α is the scaling factor, $J(q)$ is the analytic Jacobian matrix of the manipulator, $R_\alpha^{-1} = (\alpha R)^{-1}$, $x \in R^2$ stands for the end-effector transformation from robot base to camera base. In the screen coordinate frame, the robot position is captured with the following position, given in pixels,

$$x = \alpha_0 \frac{\lambda_f}{\lambda_f - z} \begin{bmatrix} -1 & 0 \\ 0 & 1 \end{bmatrix} R_0 f(q) + \beta$$
$$= \alpha R f(q) + \beta \qquad (3)$$

where α_0 is the scaling parameter[1], $R_0 \in R^{2 \times 2}$ stands for the 2×2 upper square matrix of $R_\theta \in SO(3)$, that is

$$R_0 = \begin{bmatrix} -\cos(\theta) & \sin(\theta) \\ \sin(\theta) & \cos(\theta) \end{bmatrix} \qquad (4)$$

$$\alpha = \alpha_0 \frac{\lambda_f}{\lambda_f - z} < 0 \qquad (5)$$

$$R = \begin{bmatrix} \cos(\theta) & -\sin(\theta) \\ \sin(\theta) & \cos(\theta) \end{bmatrix} \qquad (6)$$

$$\beta = \alpha_0 \frac{\lambda_f}{\lambda_f - z} \begin{bmatrix} {}^vO_{b1} \\ {}^vO_{b2} \end{bmatrix} + \begin{bmatrix} u_c \\ v_c \end{bmatrix} \qquad (7)$$

where λ_f is the focal lenght along the optical axis, z stands for the depth of field, u_c, v_c stands for the cartesian position in image coordinates, and ${}^vO_{b1}, -{}^vO_{b2}$ stands for the offset between optical axis and $\vec{Z}$ of the robot base

---

[1]Without loss of generality, α_0 can be considered as a 2×2 scaling matrix.

IV. DECENTRALIZED DYNAMIC VISUAL SERVOING

Consider the following definitions [7]

$$\dot{\bar{q}}_r = \bar{J}^{-1}\bar{R}_\alpha^{-1}\dot{x}_r \qquad (8)$$

where $\bar{J}^{-1}$ and $\bar{R}_\alpha^{-1}$ stand for an estimate of the inverse of the analytical Jacobian J^{-1} and the inverse of the modulated rotational matrix R_α^{-1}, respectively. Thus, an uncalibrated joint error manifold $\bar{s}_q$ vector is

$$\bar{s}_q = \dot{q} - \dot{\bar{q}}_r \qquad (9)$$

The nominal reference $\dot{x}_r$ of (8) is given by

$$\dot{x}_r = \dot{x}_d - \lambda(t)\Delta x + s_d - K_i \upsilon \qquad (10)$$
$$\dot{\upsilon} = sgn(s_\delta) \qquad (11)$$

where x_d and $\dot{x}_d$ denote the desired position and velocity of the end-effector with respect to the image frame, respectively, that is the image of the robot in the pixels, and

$$s_\delta = s - s_d \qquad (12)$$
$$s = \Delta \dot{x} + \lambda(t)\Delta x \qquad (13)$$
$$s_d = s(t_0) \exp^{-\kappa t} \qquad (14)$$

with the integral feedback gain $K_i = K_i^T \in R_+^{n \times n}$ whose precise lower bound is to be defined yet; $\lambda(t)$ is a time varying feedback gain; $\kappa > 0$; the $sgn(y)$ is the entrywise discontinuous $signum(y)$ function of $y \in R^n$; $\Delta x = x - x_d$ is the image-based end-effector position tracking error in pixels; $s_d \in C^1$ and $s_\delta(t_0) = 0 \ \forall \ t$.

Theorem 1: Consider a robot manipulator (1) subject to unknown robot dynamics and unknown camera parameters in closed loop with the following sliding PID visual servoing scheme

$$\tau = -K_d \bar{s}_q \qquad (15)$$

with $\lambda(t)$ of (10) given by

$$\lambda(t) = \lambda_0 \frac{\dot{\xi}}{(1 - \xi) + \delta} \qquad (16)$$

where $\lambda_0 = 1 + \epsilon$, for small positive scalar ϵ such that λ_0 is close to 1, and $0 < \delta \ll 1$. The generator $\xi = \xi(t) \in C^2$ must be provided by the user so as to ξ goes from $0 \rightarrow 1$ in finite time t_g. The $\dot{\xi} = \dot{\xi}(t)$ is a bell shaped derivative of ξ such that $\dot{\xi}(t_0) = \dot{\xi}(t_g) \equiv 0$. Then, the closed-loop system yields finite-time convergence $\Delta x(t_g) = 0, \Delta \dot{x}(t_g) = 0$, for an arbitrary given finite time $t = t_s > 0$ provided that

K_d and K_i are tuned large enough, for small enough initial error conditions.

Proof. The stability analysis can be found in [7].

Remark 1: This control law guarantees a very fast local tracking, for the dynamic model of nonlinear robot dynamics. However, this has been derived for the continuous domain, and since the CCD camera introduces a latency impossible to neglect, then there arises the important issue of two time scaling in the closed loop system. That is, the servo control loop should run very fast, say at $1\ KHz$, while the camera delivers images at slower rate, say $33Hz$. Thus, how can we implement this control system? The continuous domain controller is very powerful, in a sense that delivers high performance tracking (simple control structure, low computational cost and fast tracking regime), thus we would like to preserve this structure. Therefore, we need to introduce somehow a predictor which delivers estimated images at faster rate, ideally, also at $1\ KHz$. To this end, in this paper, we present an adaptive predictor and show the experimental validation.

V. PREDICTION OF THE END-EFFECTOR POSITION

To cope with the problem of slow refreshing rate and time delay, inherit to the CCD technology of video cameras, an estimated image based end-effector positions $\hat{x}$ were obtained using the following *Projection algorithm* [5]

$$\hat{x}_i(k) = \hat{a}_i(k)^T M_i(k-1) \tag{17}$$

$$\hat{a}_i(k) = \hat{a}_i(k-1) + \frac{\gamma M_i(k-2)\varepsilon_i(k)}{1 + M_i(k-2)^T M_i(k-2)} \tag{18}$$

$$\varepsilon_i(k) = x_i(k-1) - \hat{a}_i(k-1)^T M_i(k-2) \tag{19}$$

where $X(k)$ represents the value of variable X in the instant k, $\hat{V}$ stands for the estimated of vector V, $\hat{a}_i = [\hat{a}_{i_1}...\hat{a}_{i_n}]^T$, with $i = u, v$ for each dimension of vector x, and n stands for the among of previous states to be considered for the prediction, $\gamma = diag[\gamma_1...\gamma_n]$ is the algorithm gain, with $\gamma_j > 0$. It is supposed that x satisfies the following autoregressive model

$$x_i(k) = a_i(k)^T M_i(k-1) + e_i(k), \tag{20}$$

where vector a_i is unknown, $e_i(k)$ represents modelling errors and is assumed to be Gaussian noise with zero mean. And finally, M_i is a vector of positions x_i as follows

$$M_i(k-1) = [x_i(k-1)...x_i(k-n)]^T. \tag{21}$$

This technique has been extensively validated in a comparative simulation study with the Smith Predictor and Extended Kalman Filter, giving the best results this adaptive approach.

VI. REMARKS ON THE CONTROLLER

A. PID-like Structure

The controller (15) can be written as follows

$$\begin{aligned}
\tau = &- K_d \bar{s}_q \\
= &- K_d J^{-1} R_\alpha^{-1} \dot{q} \\
&+ K_d (\bar{J}^{-1} \bar{R}_\alpha^{-1} \{x_d - \lambda \Delta x + s(t_0) \exp^{-\kappa t} \\
&- K_i \int_{t0}^{t} sgn(s_\delta)\})
\end{aligned} \tag{22}$$

Finally, (22) exhibits a PID-like structure plus vanishing term $K_d s(t_0) \exp^{-\kappa t}$ and a nonlinear compensation input $K_d \{\bar{J}^{-1} \bar{R}_\alpha^{-1} - J^{-1} R_\alpha^{-1}\} \dot{x}_d$ as follows

$$\begin{aligned}
\tau = &- K_p(t) \Delta x - K_v(t) \Delta \dot{x} - K_{int} \int_{t0}^{t} sgn(s_\delta) dt \\
&\Sigma_1(t) + \Sigma_2(t)
\end{aligned} \tag{23}$$

where

$\Sigma_1(t) = K_d s(t_0) \exp^{-\kappa t}$ is an exponentially vanishing signal which is useful for inducing a sliding mode for any initial condition, and $\Sigma_2(t) = K_d \{\bar{J}^{-1} \bar{R}_\alpha^{-1} - J^{-1} R_\alpha^{-1}\} \dot{x}_d$ compensates for uncalibrated visual information. The state dependant feed-
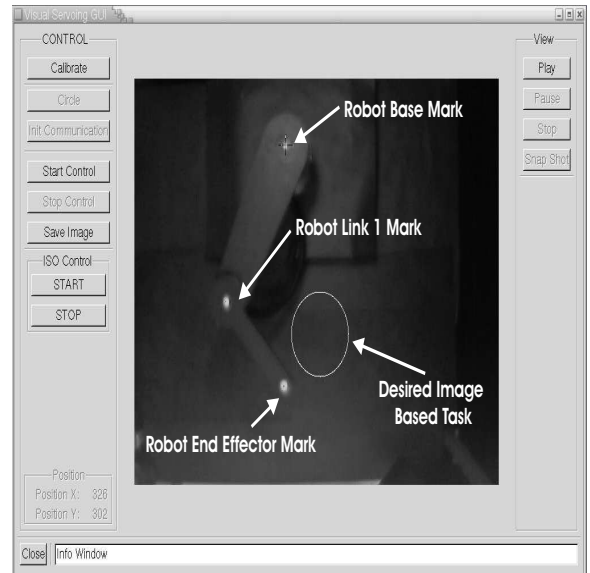

Fig. 1. Experimental system, seen by the GUI.

back gains are

$$K_p(t) = K_d J^{-1} R_\alpha^{-1} \lambda(t)$$
$$K_v(t) = K_d J^{-1} R_\alpha^{-1}$$
$$K_{int} = K_d K_i$$

Notice that these feedback gains depend on q through the *real* Jacobian and real calibration parameters.

B. Simple Structure

It is evident the simple structure of this controller, only an estimate of the composition of the manipulator Jacobian matrix, the rotation matrix and the scaling and depth parameters is required.

VII. SIMULATIONS AND EXPERIMENTAL RESULTS

A. Simulations

A two-rigid link, planar robot is considered, with a CCD camera (see parameters in Tables I and II). All inertial parameters of the robot arm and all parameters of the camera, including depth of field of view, are unknown. The endpoint of the manipulator is requested to draw a circle in image space defined with respect to the vision frame $x_d = (x_{d1}, x_{d2})^T = (0.1\cos\omega t + 0.25, 0.1\sin\omega t + 0.15)$, where $\omega = 0.5$ rad/sec. Simulations are carried in Matlab 6.0, with RungeKutta45 as the numerical solver, at 1 ms. Results presented in Figure (6) shows exponential tracking capabilities of the control with a remarkable smooth control effort, see Fig. 6

Robot parameter	Value
Length link l_1, l_2	$0.4, 0.3\ m$
Center of gravity 1,2 l_{c1}, l_{c2}	$0.1776, 0.1008\ m$
Mass link m_1, m_2	$9.1, 2.5714\ kg$
Inertia link I_1, I_2	$0.284, 0.0212\ kgm^2$

TABLE I

ROBOT PARAMETERS.

Vision parameters	Value
Clock-wise rotation angle θ	$\frac{\pi}{2}\ rad$
Scale factor α_v	$77772\ pixeles/m$
Depth field of view z	$1.5\ m$
Camera offset ${}^v O_b$	$[-0.2\ \ -0.1]^T\ m$
Offset $\Sigma_I\ o_I$	$[0.0005\ \ 0.0003]^T\ m$
Focal length λ_f	$0.008\ m$

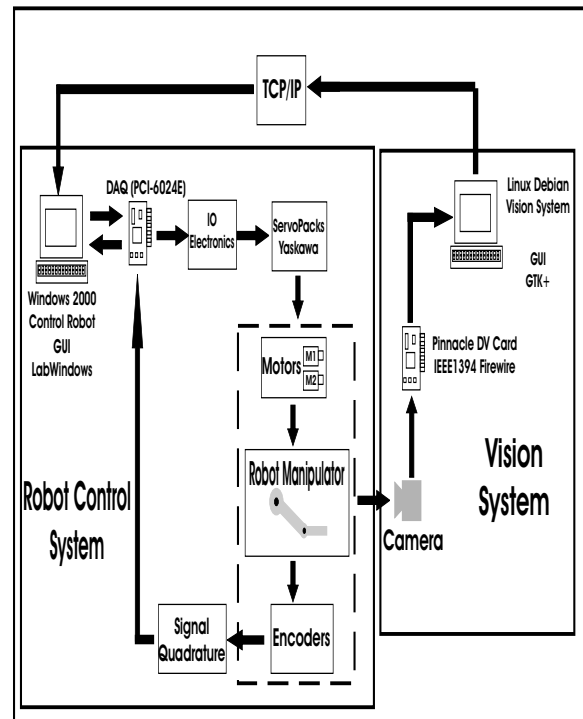TABLE II

CAMERA PARAMETERS.

Fig. 2. Flow signals of the complete visual System

B. Experimental System Setup

The system consists of two PC that deal with vision system and robot control system, a 2 DOF direct drive planar robot, designed and constructed at the institute, and finally a CCD fixed camera, as showed in Figure (1). In Figure (2) is showed the visual control schem of the experimental system. In next few lines a brief description of each part of the experimental system is given.

C. Hardware

The implementation of the vision system was done in a 1.533 Ghz AMD 1800+ processor, with 512 Mb DRAM, PC, which runs over Linux OS with a Real Time Application Interface module (Linux RTAI) to performs hard real time scheduling. A Pinnacle Studio DV PC board manages transmission of visual information on IEEE1394 ports. Visual information acquisition is done with a SONY DFW-V500 digital CCD camera with 30 fps full motion picture, which adopts the IEEE1394-1995 standard, a high speed serial bus (more than 400 $Mbit/s$). The robot control system was implemented in a 1.5 Ghz Pentium IV PC with 256 Mb DRAM memory on Windows 2000 OS. The 2 DOF planar robot is actuated by two 220V A.C. direct drive motors with integrated optical encoders.
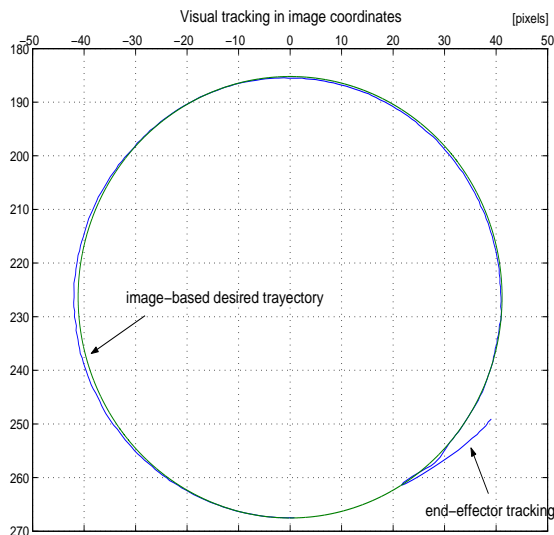
Fig. 3. End-effector tracking an image-based task. This figure shows the position error convergence, this convergence is exponential, as we can see the maximum experimental image based position error presented is $< 1.5\ pixels$

The motors are Yaskawa SGM-08A314 and SGM-04U3B4L with drivers Yaskawa Servopacks SGD-08AS and SGDA-04AS respectively. The National Instruments PCI-6024E data acquisition board was installed to handle the I/O signals.

D. Software

The visual system affords a visual tracking system and a GUI coded in a free Linux software that provides useful user tools to design the image based robot end-effector task, see Fig. 1. The visual tracking system analyze and process image data information to track special visual marks on robot end effector, robot link 1 and robot base as showed in Figure 1. The marks were chosen as circles of different radius[2]. The visual tracking system is compose of two main procedures.

In order to provide a friendly user interface in the robot control system, a GUI was developed on Lab-Windows/CVI 6.0 of National Instruments. Finally, communication between vision and robot control systems is via TCP/IP protocol.

E. Experimental Results

The desire image based task is follow a circle track with radius $r = 40\ pixels$, and centered in $(c_x, c_y) =$

[2]The selection of this marks is owing to its image properties, that is, rotational invariance.

$(360, 450)\ pixels$ referenced with the image space axes. The circle is generated with an angular velocity of $\omega = 0.628\ rad/s$. The position of the robot end effector is showed at the GUI in the visual system. The visual field of camera covers completely the robot work space and $R_1 - R_2 \parallel S_1 - S_2$, where $R_1 - R_2$, $S_1 - S_2$, stands for robot work space and image space, respectively. The capture period of camera is $30\ fps$. The positions of the robot end-effector in image coordinates were predicted as described in V. On the other hand, both joint and image velocities of the end-effector were obtained by Euler derivation from the joint positions and the predicted image positions, respectively, and then filtered with a second order Butterworth filter. The experimental results of this approach are showed in Figures (3), 4 and 5.

VIII. CONCLUSIONS

In this paper was carried out the experimental validation of the decentralized nonlinear PID-like controller for visual tracking of planar robots reported in [7]. The high performance of the controller is revealed with the experimental results, that shows the main features of the scheme: the finite-time convergency of tracking errors defined by user, the controller robustness on uncertainty of visual parameters and without dynamical knowledge, and finally, a low computational cost in its implementation. The implementation was conducted by a projection algorithm to predict the image-based position, avoiding the time delay associated with the image acquisition and processing.
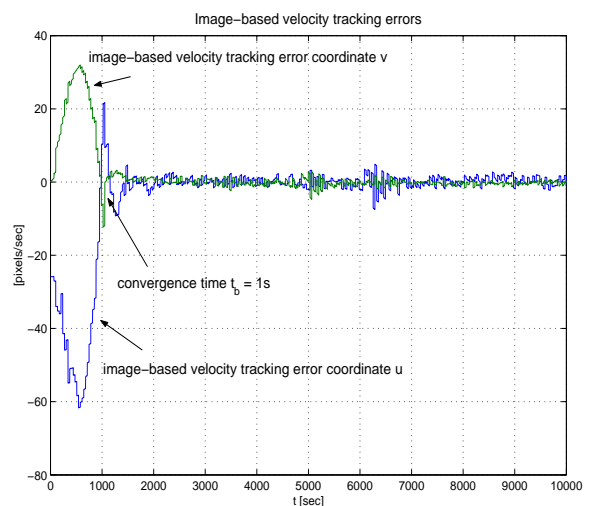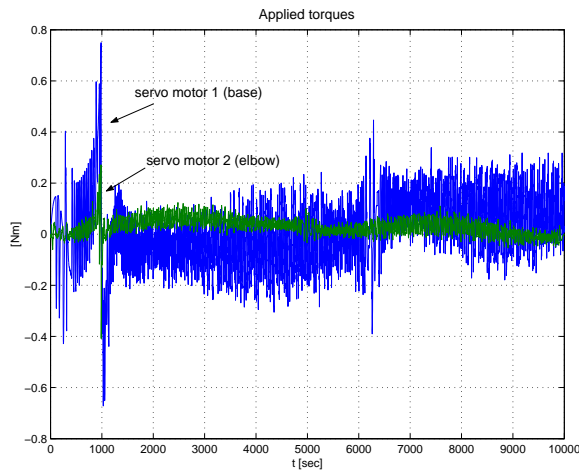

Fig. 4. Image-based velocity tracking errors.

Fig. 5.   Applied torques.

ACKNOWLEDGEMENTS

REFERENCES

[1] P. Anandan, "Computing dense displacement fields with confidence measures in scenes containing occlusion" Proceedings of SPIE, Inteligent Robots an Computer Vision, November 5-8. 1984.

[2] L. Hsu, and P. Aquino, Adaptive Visual Tracking with Uncertain Manipulator Dynamics and Uncalibrated Camera, 1999 Proc. 38th IEEE Conference on Decision and Control, pp. 1248-1253.

[3] B.E. Bishop, and M.W. Spong, Adaptive calibration and control of 2D monocular visual servo systems, IFAC Symp. on Robot Control, France, 1997.

[4] W.E. Dixon, E. zergeroglu, Y. fang, and D.M. Dawson, Object Tracking by a Robot Manipulator: Robust Cooperative Visual Servoing Approach, Proceeding of the 2002 IEEE International Conference on Robotics & Automation, 211-216.

[5] G.C. Goodwin, and K.S. Sin, "Adaptive Filtering Prediction and Control. " Prentice-Hall: Englewood Clifs, NJ, 1984.

[6] S. Hutchinson, G.D. Hager, and P.I. Corke, A Tutorial on Visual Servo Control, Trans. on Robotics and Automation, 12:651-670, 1996.
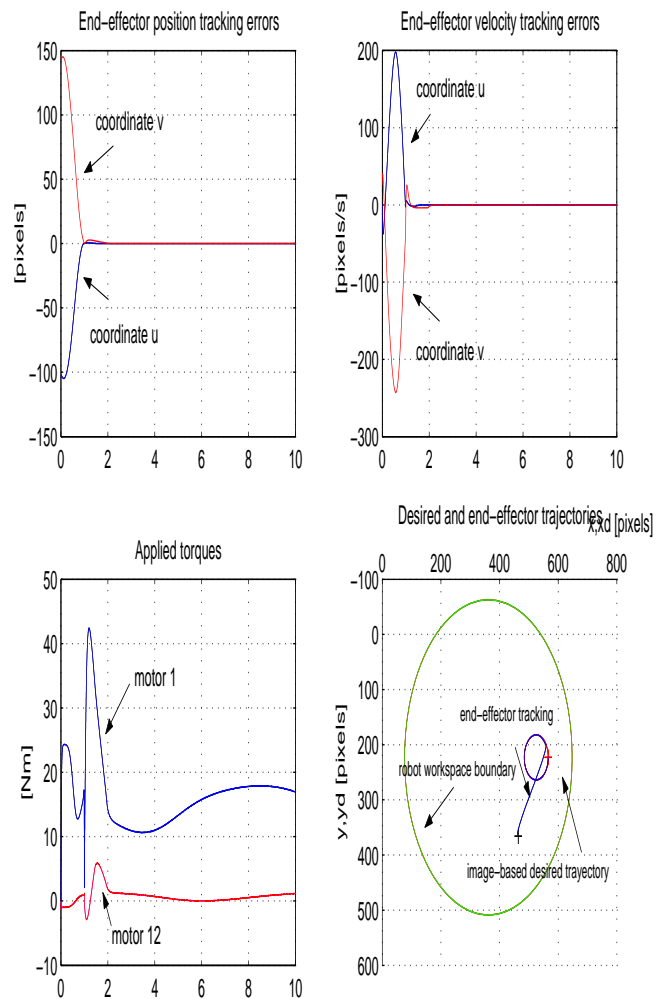

Fig. 6.   Simulation Results: Above left, u and v image tracking errors converge exponentially fast, and above right shows their corresponding velocity tracking errors. Below left shows smooth applied torques,while below right shows the resulting image phase plane circumscribed by the image robot workspace, cross mark stand for the initial point.

[7] V. Parra-Vega, J.D. Fierro-Rojas, and A. Espinosa-Romero, Uncalibrated Sliding Mode Visual Servoing of Uncertain Robot Manipulators, 2003 IEEE International Conference on Robotics and Automation, May 12 - 17, Taipei, Taiwan.

[8] Y. Shen, G. Xiang, Y.H. Liu, and K. Li, Uncalibrated visual Servoing of Planar Robots, Proceeding of the 2002 IEEE International Conference on Robotics & Automation, Washinton, D.C., 580-585.

[9] R. Y. Tsai, and R. K. Lenz, Techniques for calibration of the scale factor and image center for high accuracy 3-D machine vision metrology, IEEE Trans. Pattern Anal. Machine Intell., 1988, 10(5):713-720.

[10] E. Gortcheva, R. Garrido, E. González and A. Carvallo Predicting a moving object position for visual servoing: theory and experiments, International Journal of Adaptive Control and Signal Processing. 2001; 15:377-392.